

Article

## Power Quality Assessment in Small Scale Renewable Energy Sources Supplying Distribution Systems

Nicolae Golovanov <sup>1</sup>, George Cristian Lazaroiu <sup>1,\*</sup>, Mariacristina Roscia <sup>2</sup> and Dario Zaninelli <sup>3</sup>

<sup>1</sup> University Politehnica of Bucharest, Splaiul Independentei 313, Bucharest 060042, Romania; E-Mail: nicolae\_golovanov@yahoo.com

<sup>2</sup> Dipartimento di Progettazione e Tecnologie, Università di Bergamo, Via Marconi 6, Bergamo 24044, Italy; E-Mail: cristina.roschia@unibg.it

<sup>3</sup> Politecnico di Milano, Via La Masa 34, Milan 20156, Italy; E-Mail: dario.zaninelli@polimi.it

\* Author to whom correspondence should be addressed; E-Mail: clazaroiu@yahoo.com; Tel.: +40-21-4029-997; Fax: +40-21-4029-440.

Received: 21 November 2012; in revised form: 17 January 2013 / Accepted: 22 January 2013 /

Published: 29 January 2013

---

**Abstract:** The impact of wind turbines and photovoltaic systems on network operation and power quality (harmonics, and voltage fluctuations) is very important. The capability of the power system to absorb this perturbation is dependent on the fault level at the point of common coupling. The paper deals with power quality case studies conducted on existing renewable resources-based systems. Voltage fluctuations determined by a 0.65 MVA wind turbine are analyzed. The impact of photovoltaic systems on steady state voltage variations and current harmonics is investigated. The correlation between the generated power and the main power quality indices is highlighted.

**Keywords:** power quality; small scale renewable sources; voltage fluctuations; harmonics

---

### 1. Introduction

Renewable energy sources (RESs), with powers varying from 100 kW to a few MW, are increasingly present in electrical networks. The economic opportunities, the liberalization and the potential benefits for electrical utilities (peak shaving, support for distribution and transmission networks) are contributing to the already existing trend, leading to a more decentralized energy market [1]. The RES systems can be used in small, decentralized power plants or in large ones, they can be built with small

capacities and can be used in different locations. In isolated areas where the cost of the extension of the power systems (from the utilities' point of view) or the cost for interconnection with the grid (from the customer's point of view) are very high with respect to the cost of the RES system, these renewable sources are suitable. The RES systems are "environmentally friendly" and appropriate for a large series of applications, such as stand-alone systems for isolated buildings or large interconnected networks. The modularity of these systems make possible their expansion in the case of a subsequent load growth.

As RESs becomes more reliable and economically feasible, there is a trend to interconnect RES units to the existing utilities to serve different purposes and offer more possibilities to end-users, such as:

- a. Improving availability and reliability of electric power;
- b. Peak load shaving;
- c. Selling power back to utilities or other users;
- d. Power quality (improvement of the voltage level, without an additional regulation of reactive power).

The increasing penetration rate of RES in the power systems is raising technical problems, as voltage regulation, network protection coordination, loss of mains detection, and RES operation following disturbances on the distribution network [2]. These problems must be quickly solved in order to fully exploit the opportunities and benefits offered by the RES technologies. As the RES are interconnected to the existing distribution system, the utility network is required to make use of RES maintaining and improving the supply continuity and power quality delivered to the customers [3].

The present paper deals with the experimental investigation of the impact of renewable sources on power quality. The voltage fluctuations generated by wind turbines are analyzed, during continuous operation as well as for generator interconnection. The steady state voltage variation at the point of common coupling due to the PV system connection is analyzed for sunny and cloudy days. The PV systems interfaced to the main grid with the help of inverters are injecting harmonics in the 50 Hz grid. The correlation between the PV generated power and the main harmonic distortion indices is presented.

In particular, in Section 2, the power quality in distributed generation systems is discussed. Section 3 is devoted to the voltage fluctuations determined by a 0.65 MVA wind turbine. In Section 4, the investigation of steady state voltage variations at the point of common coupling is carried out. Current harmonics injected in the 50 Hz grid are experimentally illustrated in Section 5. Finally, conclusions are given in Section 6.

## 2. Power Quality in Distributed Generation Systems

Nowadays, wind generation is developing in the whole world. As these renewable sources are increasingly penetrating the power systems, the impact of the wind turbines on network operation and power quality is becoming important [4]. Due to the output power variations of wind turbines, voltage fluctuations are produced. The capability of the power system to absorb this perturbation is dependent on the fault level at the point of common coupling. In weak networks or in power systems with a high wind generation penetration, the integration of these sources can be limited by the flicker level that must not exceed the standardized limits.

The photovoltaic (PV) installations, interconnected to the mains supply, can be single-phase connected (photovoltaic installations with capacity less than 5 kW) or three-phase connected

(photovoltaic installations with capacity greater than 5 kW). The produced power, characterized by high randomness, can determine a low power quality with important perturbing emissions in the power systems. These effects are less observed at the point of common coupling (PCC), where the short-circuit level is high. Increasing the installed photovoltaic capacity, the electromagnetic disturbances become important. The direct-coupled PV systems, without electrical energy storage, inject in the power system a generated power that follows the intermittency of the primary energy source. In this case, important voltage variations can occur at the PCC. The connection of PV systems to the low voltage grid can determine voltage variations and harmonic currents [5,6].

### 3. Voltage Fluctuations (Flicker Effect)

The possibility for reducing voltage fluctuations determined by wind turbines requires the establishment of some regulations, when and how often the wind turbines operators can start or vary the output power. In some cases, voltage fluctuations problems can be solved without a detailed study, by simply adjusting a control element, until the voltage flicker level is reduced below the standardized value [7,8]. In some other cases, complex analysis limiting flicker is requested. Determination of voltage fluctuations due to output power variations of renewable sources is difficult, because they depend on the source's type, generator's characteristics and network impedance.

For the case of wind turbines, the long term flicker coefficient  $P_{lt}$  due to commutations, computed over a 120 min interval and for step variations, is given by Equation (1) [9]:

$$P_{lt} = \frac{8}{S_{sc}} \cdot N_{120}^{0.31} \cdot k_f(\psi_{sc}) \cdot S_r \quad (1)$$

where  $N_{120}$  is the number of possible commutations in a 120 min interval,  $k_f(\psi_{sc})$  is the flicker factor defined for angle  $\psi_{sc} = \arctan(X_{sc}/R_{sc})$ ,  $X_{sc}$  is the reactance of short-circuit network impedance,  $R_{sc}$  is the resistance of short-circuit network impedance  $S_r$  is the rated power of the installation, and  $S_{sc}$  is the fault level at point of common coupling (PCC). In the present paper, the power system, where the wind farm is connected, is simulated through  $S_{sc}$  and  $\psi_{sc}$ . The propagation of perturbations within the electrical network is not investigated.

For a 10 min interval, the short-term flicker  $P_{st}$  is defined by Equation (2) [9]:

$$P_{st} = \frac{18}{S_{sc}} \cdot N_{10}^{0.31} \cdot k_f(\psi_{sc}) \cdot S_r \quad (2)$$

where  $N_{10}$  is the number of possible commutations in a 10 min interval.

The values of flicker indicator for wind turbines, due to normal operation, can be evaluated using flicker coefficient  $c(\psi_{sc}, v_a)$ , dependent on average annual wind speed,  $v_a$ , in the point where the wind turbine is installed, and the phase angle of short circuit impedance,  $\psi_{sc}$ :

$$P_{st} = P_{lt} = c(\psi_{sc}, v_a) \frac{S_r}{S_{sc}} \quad (3)$$

The flicker coefficient  $c(\psi_{sc}, v_a)$  for a specified value of the angle  $\psi_{sc}$ , for a specified value of the wind speed  $v_a$  and for a certain installation is given by the installation manufacturer, or can be determined experimentally based on standard procedures. Depending on the voltage level where the wind generator (wind farms) is connected, the angle  $\psi_{sc}$  can take values between  $30^\circ$  (for the medium

voltage network) and  $85^\circ$  (for the high voltage network). Flicker evaluation is based on the IEC standard 61000-3-7 [8], which provides guidelines for emission limits for fluctuating loads in medium and high voltage networks. Table 1 lists the recommended values.

**Table 1.** Flicker planning levels for medium voltage (MV) and high voltage (HV) networks.

Flicker severity factor	Planning levels	
	MV	HV
$P_{st}$	0.9	0.8
$P_{lt}$	0.7	0.6

The flicker evaluation determined by a wind turbine of 0.65 MVA is analyzed. The wind turbine has a tower height of 80 m, the rotor diameter is 47 m, and the swept area is  $1,735 \text{ m}^2$ . The electrical energy production during the months of February and March were 127,095 kWh and 192,782 kWh, respectively. The average wind speed, measured at 60 m height, during February was 6.37 m/s, while during March it was 7.32 m/s. The measurement data for the month of February are reported in Table 2. The experimental data for the month of March are reported in Table 3.

**Table 2.** Wind turbine experimental data during the month of February.

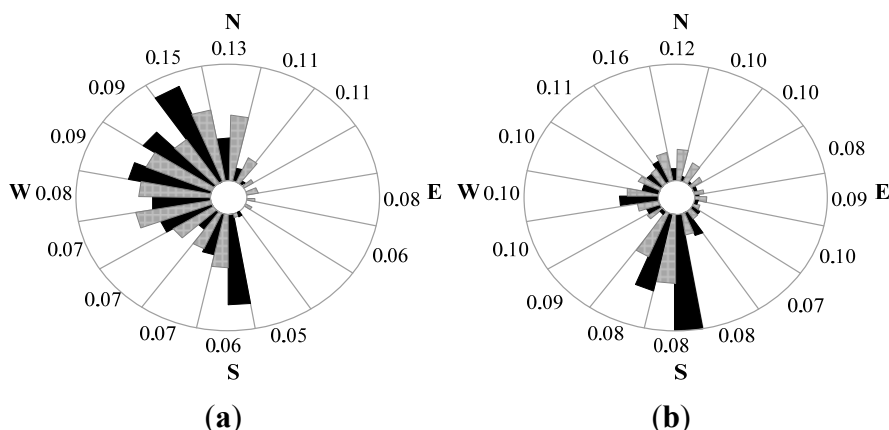
Average wind speed at hub height (m/s)		
60 m	50 m	40 m
6.37	6.30	6.045

**Table 3.** Wind turbine experimental data during the month of March.

Average wind speed at hub height (m/s)		
60 m	50 m	40 m
7.32	7.165	6.95

The wind rose graph presented in Figure 1 illustrates the percent time and percent energy in each direction sector. The wind rose is divided in 16 sectors, each one of  $22.5^\circ$ . The outer circle represents 30% of the total energy or time. The black areas represent the percent of total wind energy, and the shaded areas illustrate the percent of total time. The outer values represent the intensity of wind turbulence in the investigated location. The turbulence intensity  $\sigma_0$  is defined as the ratio between the standard deviation  $\sigma_v$  of wind speed and the average wind speed in a specified time interval. In the case of reduced wind speeds, high turbulence intensities can lead to an increase of the produced power. In practice, for the nominal wind speed, large turbulence intensities can reduce the produced power as the control systems difficulty follow the sudden and large wind speed variations. Figure 1a illustrates the wind rose, at 60 m height, of the wind turbine during February. As it can be seen, the prevailing winds in this area come from the west, south and northwest. Figure 1b illustrates the wind rose, at 60 m height, of the wind turbine during March. As it can be seen, the prevailing winds in this area come from the west, south and southwest.

**Figure 1.** Wind rose for (a) the month of February and (b) for the month of March.



Measurements were conducted on the wind turbine system described in this paper. The variation of wind speed over the monitoring period is shown in Figure 2. The variation of turbine output power is shown in Figure 3. The intermittent character of the produced power is clearly visible. The tower shadow effect for the wind generator determines a variation of the absorbed energy, which is measured as a power variation at generator terminals. Figure 4a shows the wind generator, while Figure 4b illustrates the tower shadow effect corresponding variation of the generator output power.

**Figure 2.** Wind speed variation during the one month monitoring period.

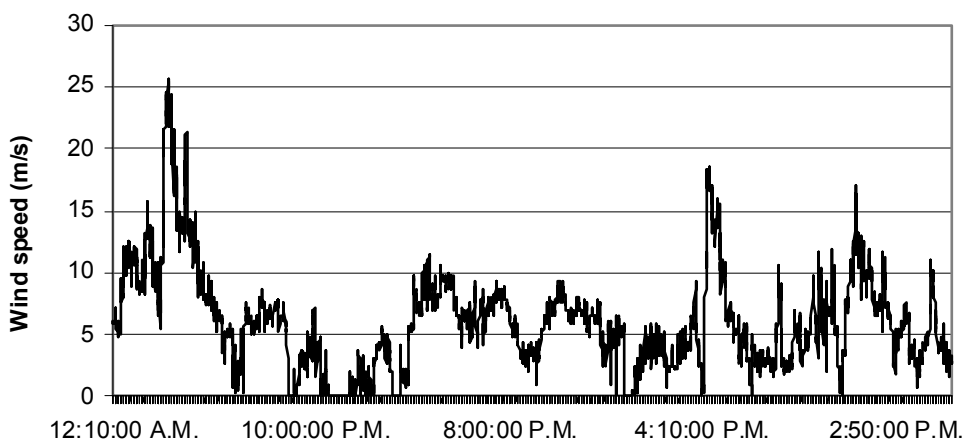


**Figure 3.** Turbine output power variation during the one month monitoring period.

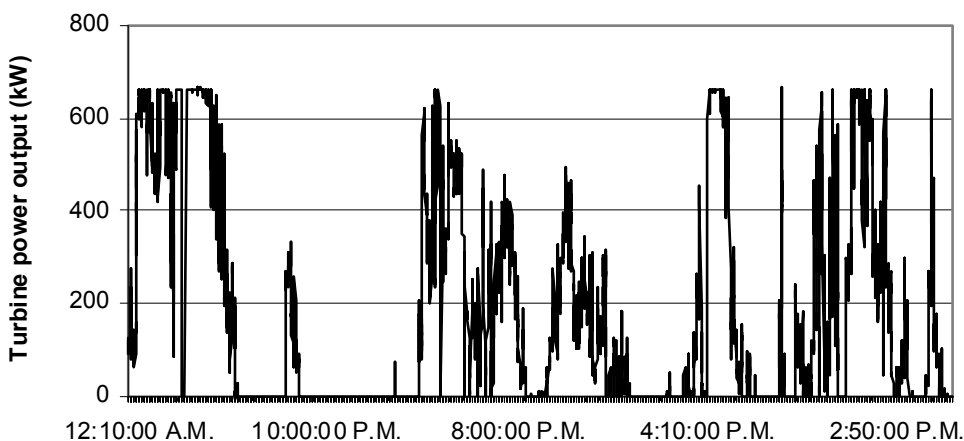
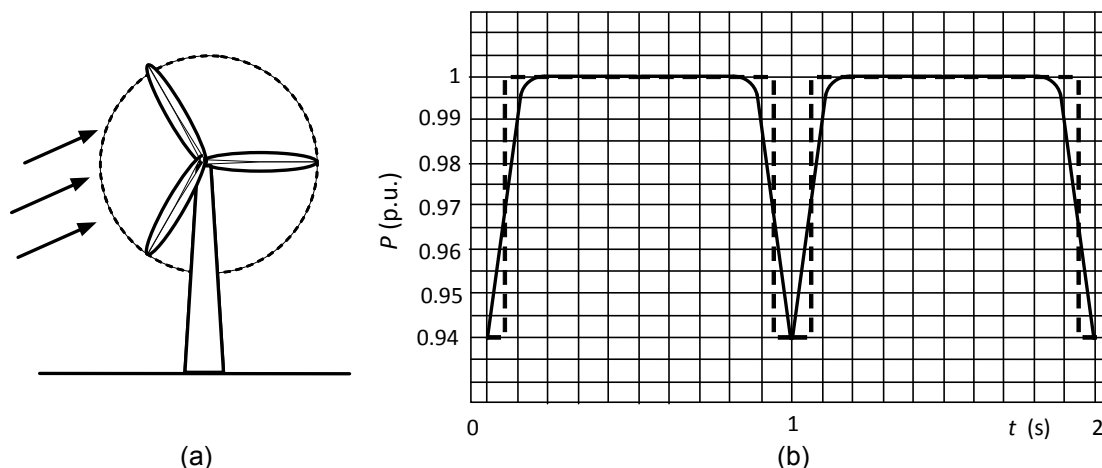


**Figure 4.** Tower shadow effect: (a) wind generator and (b) output power variation.



The measured values of the flicker coefficient  $c(\psi_{sc}, v_a)$  for different values of the annual average wind speed  $v_a$  and for different network impedance angle  $\psi_{sc}$  are reported in Table 4. Table 5 gives the flicker coefficient  $k_f$  values for voltage step variations, for the same wind generator.

**Table 4.** Values of the flicker factor for various values of the wind speed  $v_a$  and for various angles  $\psi_{sc}$ .

Annual wind speed $v_a$ (m/s)	Network impedance angle $\psi_{sc}$ (°)			
	30°	50°	70°	85°
6	3.1	2.9	3.6	4.0
7.5	3.1	3.0	3.8	4.2
8.5	3.1	3.0	3.8	4.2
10	3.1	3.1	3.8	4.2

**Table 5.** Values of the flicker factor  $k_f$ .

Conditions of operation		Network impedance angle $\psi_{sc}$ (°)			
		30°	50°	70°	85°
Flicker factor $k_f$ for	With start at minimum speed	0.02	0.02	0.01	0.01
voltage step variations	With start at rated speed	0.12	0.09	0.06	0.06

Note: Installation is sized for  $N_{10} = 3$ ;  $N_{120} = 35$ .

The computations based on the values reported in Tables 4 and 5 lead to the flicker indicator values:

1. Continuous operation, annual average wind speed  $v_a = 7.5$ , interconnection with the medium voltage network ( $\psi_{sc} = 50^\circ$ ,  $S_{sc} = 300$  MVA,  $S_r = 0.65$  MVA), given by Equation (4):

$$P_{st} = P_{lt} = \frac{S_r}{S_{sc}} \cdot c(\psi_{sc}, v_a) = \frac{0.65}{300} \cdot 3 = 0.0065 \tag{4}$$

2. Generator interconnection at minimum speed of the wind turbine, given by Equation (5):

$$P_{st} = 18 \cdot N_{10}^{0.31} \cdot k_f(\Psi_{sc}) \cdot \frac{S_r}{S_{sc}} = 18 \cdot 3^{0.31} \cdot 0.02 \cdot \frac{0.65}{300} = 0.00109$$

$$P_{tt} = 8 \cdot N_{120}^{0.31} \cdot k_f(\Psi_{sc}) \cdot \frac{S_r}{S_{sc}} = 8 \cdot 35^{0.31} \cdot 0.02 \cdot \frac{0.65}{300} = 0.00104 \quad (5)$$

3. Generator interconnection at rated speed of the wind turbine, given by Equation (6):

$$P_{st} = 18 \cdot N_{10}^{0.31} \cdot k_f(\Psi_{sc}) \cdot \frac{S_r}{S_{sc}} = 18 \cdot 3^{0.31} \cdot 0.09 \cdot \frac{0.65}{300} = 0.0049$$

$$P_{tt} = 8 \cdot N_{120}^{0.31} \cdot k_f(\Psi_{sc}) \cdot \frac{S_r}{S_{sc}} = 8 \cdot 35^{0.31} \cdot 0.09 \cdot \frac{0.65}{300} = 0.0047 \quad (6)$$

Due to the output power variations of the wind turbines, voltage fluctuations are produced. Voltage fluctuations are produced due to the wind turbine switching operations (start or stop), and due to the continuous operation. The presented voltage fluctuations study, made for one turbine, becomes necessary in large wind farms as the wind power penetration level increases quickly.

#### 4. Steady State Voltage Variations

The variable nature of solar radiation, the weather changes or passing clouds can cause variations of PV output power [10]. The variation of the power produced by a 30 kW PV system is illustrated in Figure 5. Figure 6a shows the generation power in a sunny day, while Figure 6b illustrates the generation power in a cloudy day. Typically, the photovoltaic panels installed on house roofs generate up to 5 kW. The sources are normally connected through a single-phase inverter to the low voltage supply system [11].

The connection of these variable renewable sources can cause a voltage rise at PCC and in the grid. The utility has the general obligation to ensure that customer voltages are kept within prescribed limits. A voltage variation  $\Delta V$  between  $V_{max}$  and  $V_{min}$ , can appear on short periods. This voltage variation can highly stress the electrical devices supplied by the power system, and in particular the owner of the photovoltaic facility (as shown in Figure 7). Figure 7 illustrates the possible case of a summer mid-day, when the load downstream PCC is relatively small and the PV output power exceeds the demand.

**Figure 5.** Variation of PV system power output during a month.

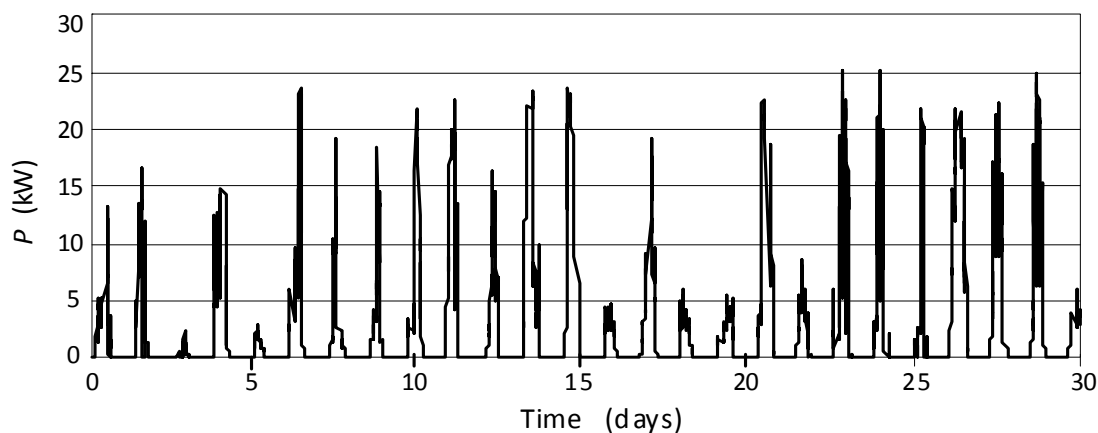


**Figure 6.** Variation of PV system power output during: (a) sunny day and (b) cloudy day.

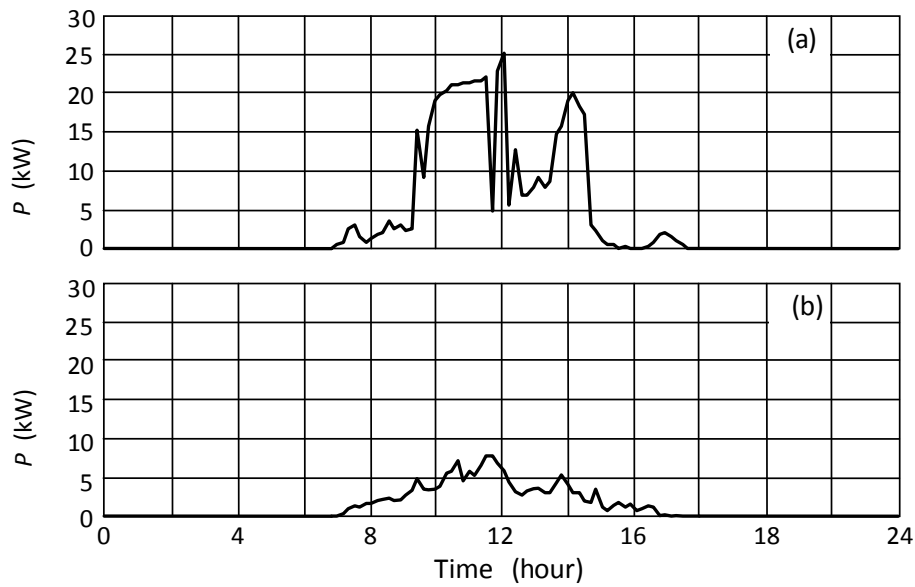
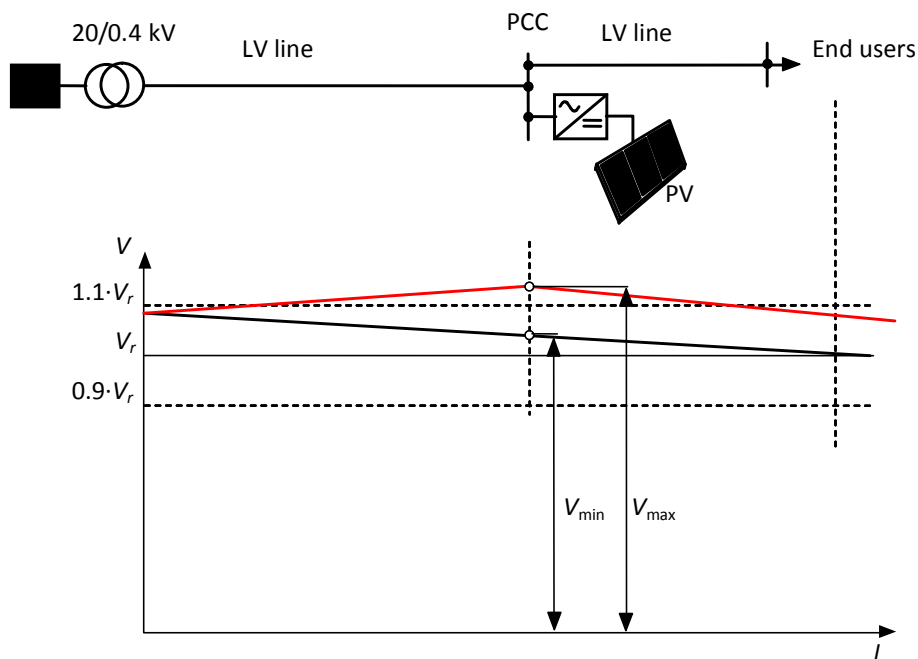


**Figure 7.** Influence of PV on voltage level: without PV source generating (black line); with PV source generating (red line).



The voltage variations can affect the characteristics of the electrical equipment and household appliances (loss of the guaranteed performances, modifications of the efficiency) leading in some cases even to the interruption of operation [12]. The voltage variation at PCC can be expressed as:

$$\Delta V = \frac{S_{PV}}{S_{sc}} \cdot \cos(\psi_{sc} - \varphi) \tag{7}$$

where  $S_{PV}$  is the power produced by PV,  $S_{sc}$  is the short circuit power at PCC,  $\psi_{sc} = \arctan(X/R)$  is the angle of the network short circuit impedance,  $\varphi$  is the phase angle of the PV output current (we

consider that the electric quantities are sinusoidal) [12]. In existing power systems, there are measures such that the line voltage to be sinusoidal. In Equation (7), the system harmonics are not considered.

The analysis of Equation (7) highlights that limiting the voltage variation  $\Delta V$  requires a careful analysis of the grid where the PV installation is connected. A power system characterized by a high short-circuit current (high short-circuit power) and a small angle  $\psi$  will be characterized by reduced voltage variations at PCC. For the medium voltage network ( $\psi \cong 50^\circ$ ) and the low voltage network ( $\psi \cong 30^\circ$ ), with small short-circuit powers, especially if the PCC is far from the substation point, large voltage variations may occur caused by PV installation of large capacity.

At low and medium voltage levels, the utilities have established limits for the amplitude of the voltage variations, which must not be exceeded during normal operation. Due to the statistical nature of the steady state voltage variations, the EN 50160 standard stipulates statistical limits [7]. In some countries the limit  $\pm 10\%$  established in EN 50160 is applied, while other current guidelines, elaborated in different countries, impose more restrictive limits for the voltage variations both for the light load as well as for the heavy load conditions, e.g.,  $\pm 6\%$  [13]. The relevant variations of the voltage will overlap the voltage's variations caused by load modification and can lead to the widening of the voltage admissible bands.

## 5. Current Harmonic Perturbations

In order to connect PV power systems with the grid, an inverter that transforms the DC output power of the PV to the 50 Hz AC power is required. The large scale PV systems are interconnected to the main grid with pulse width modulated three-phase inverters [14]. These inverters, equipped with a grid-side filter, have a small harmonic contribution (the total current harmonic distortion, *THDI*, is small), and thus the influence on voltage waveform at PCC is negligible. The small capacity PV systems are interconnected to the main grid with the help of simple single-phase inverters, which can cause important current harmonics. General requirements can be found in standards, especially those for the interconnection of distributed generation systems to the grid and for photovoltaic systems [1,15]. In the standard IEEE 1547, the harmonic current injection of PV at the PCC must not exceed the limits stated in Table 6.

**Table 6.** Main parameters for the PV system used in the simulation.

Individual harmonic order	$h < 11$	$11 \leq h < 17$	$17 \leq h < 23$	$23 \leq h < 35$	$35 \leq h$	TDD
Percent (%)	4	2	1.5	0.6	0.3	5

Note: TDD—Total demand distortion.

The harmonic spectrum is a function of inverter topology, switching frequency, control, *etc.* The measurements were conducted for a particular case of a photovoltaic plant connected to the main supply through a 6-pulse converter. The influence of converter configuration on harmonic spectrum was not analyzed. The experimental measurements reveal high values, but not relevant, of THDI. The establishment of an indicator that better illustrates the perturbations at PCC, during the operation period of renewable sources, is proposed. The function of photovoltaic systems is accompanied by the injection of some harmonic perturbation into the grid, with a total harmonic distortion factor dependent on the generated power.

Figure 8 illustrates the correlation between the generated power and total current harmonic distortion factor *THDI*, for one monitored day (the 6th day of the monitoring period shown in Figure 5). The analysis of the total harmonic distortion factor has to consider that, for high variability installations, the large *THDI* values can lead to inappropriate conclusions. The total harmonic factor is related to the fundamental component of the electric current  $I_1$ :

$$THDI = \frac{\sqrt{\sum_{h=2}^{\infty} I_h^2}}{I_1} \tag{8}$$

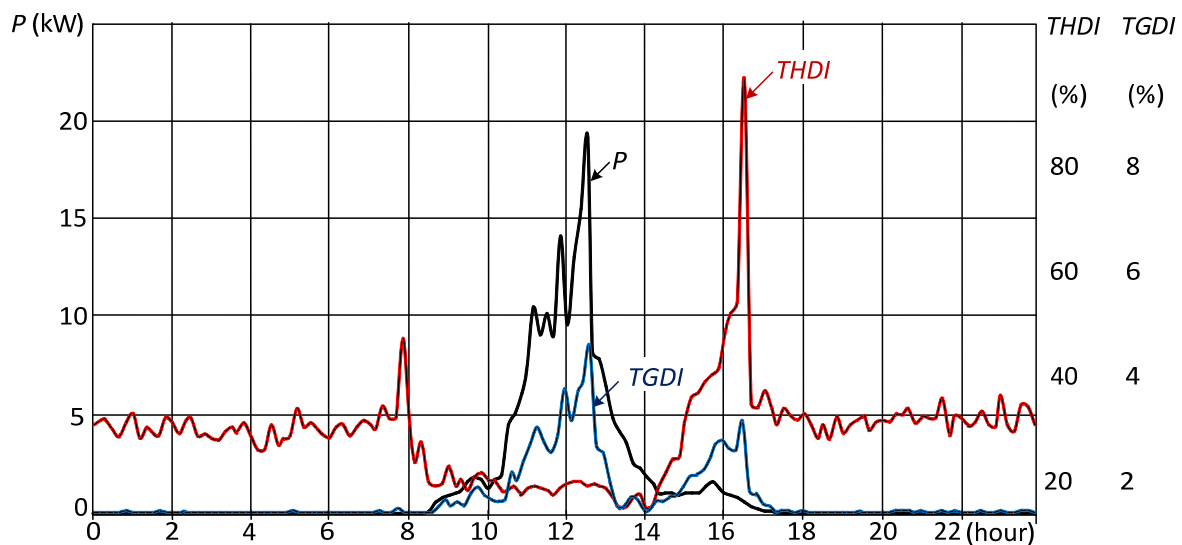
For the periods with low irradiation (especially during the morning and evening periods), the electric current injected into the grid presents a reduced fundamental component, resulting in a high distortion factor. As the electrical current has small values, the voltage drops in the power system are negligible, and thus the voltage waveform at PCC is not affected.

For assessing the operation of PV installations in terms of harmonic disturbances injected at PCC, the use of a new indicator *Total Generator Distortion Index (TGDI)* is proposed. This indicator is useful for high variability sources, which is related to the rated fundamental current of photovoltaic system  $I_r$ :

$$TGDI = \frac{\sqrt{\sum_{h=2}^{\infty} I_h^2}}{I_r} \tag{9}$$

where the rated current  $I_r$  is established and indicated for pure sinusoidal measures (a constant current value of the installation).

**Figure 8.** Correlation between the generated power, the total current harmonic distortion factor *THDI* and the total generator distortion index *TGDI*.



The relation between TGDI and THDI can be expressed as:

$$TGDI = \frac{THDI}{\sqrt{1+(THDI)^2}} \cdot \frac{I}{I_r} \quad (10)$$

We consider that the rated current  $I_r$ , established by the plant manufacturer, has a constant value for pure sinusoidal measures; the current  $I$  is the measured electrical current (inclusive all harmonics). In this paper, it is considered that harmonics are determined by converter at the interconnection point with the main supply. When the generated power is high (large value of RMS electrical current), the fundamental current is high and the  $THDI$  is small [16,17]. For small generated powers, the fundamental current is small and the  $THDI$  is high. From a practical point of view, this fact is not highly important as the small current values do not influence the voltage quality at point of common coupling. The analysis of waveforms illustrated in Figure 8 shows that the indicator  $TGDI$  better defines the effect of harmonics into the power grid, with a variation corresponding to the power injected into the network and which determines the voltage waveform at PCC, without transmitting insignificant information for the periods with very low generation. The  $THDI$  values were measured for a winter day, while the  $TGDI$  values were computed based on the conducted measurements.

The interconnection of the PV system to the main grid must not determine the total harmonic factor to exceed the stipulated values, which can occur especially when the PV system is generating the maximum power output.

## 6. Conclusions

The voltage flicker due to the output power variations, both for the wind turbine switching operations (start or stop), as well as for the continuous operation is analyzed. The voltage flicker study becomes necessary as the wind power penetration level increases quickly. The connection of variable renewable sources can determine a voltage rise at PCC, which can influence the characteristics of the electrical equipment and household appliances. The photovoltaic sources, connected to the power system through power electronic converters, can pollute the electrical network with harmonic components that must not exceed the stipulated limits. Harmonic indices correlated with the generating power are proposed and monitored for the PV installations. The analysis can be conducted for other cases of distributed generators, if there are interconnected with the mains through power electronics converters.

## References

1. *IEEE Standard 1547-2003: IEEE Standard for Interconnecting Distributed Resources with Electric Power Systems*; IEEE: Piscataway, NJ, USA, 2003.
2. Jenkins, N.; Allan, R. *Embedded Generation*; The Institution of Electrical Engineers: London, UK, 2000; pp. 49–85.
3. Dugan, R.C.; Beaty, H.W.; McGranaghan, M.F. *Electrical Power Systems Quality*; McGraw-Hill: New York, NY, USA, 1996; pp. 1–8.
4. Golovanov, N.; Lazaroiu, G.C.; Manole, A.; Roscia, M.; Zaninelli, D. Wind Farms Access to the Romanian Transport System. In *Proceedings of the IEEE Power Systems Conference & Exposition*, Seattle, WA, USA, 15–18 March 2009; pp. 1–6.

5. Golovanov, N.; Lazaroiu, G.C.; Roscia, M.; Zaninelli, D. Steady State Disturbance Analysis in PV Systems. In *Proceedings of the IEEE Power Engineering Society General Meeting*, Denver, CO, USA, 17–21 June 2004; pp. 1–6.
6. Gagliardi, F.; Iannone, F.; Lazaroiu, G.C.; Roscia, M.; Zaninelli, D. Sustainable Building for the Quality of Power Supply. In *Proceedings of the IEEE PowerTech Conference 2005*, Sankt Petersburg, Russia, 27–30 June 2005; pp. 1–6.
7. *Standard EN 50160:2010: Voltage Characteristics of Electricity Supplied by Public Distribution Systems*; CENELEC: Brussels, Belgium, 2010.
8. *IEC 61000-3-7: Assessment of Emission Limits for the Connection of Fluctuating Load Installation to MV, HV and EHV Power Systems*; IEC: Geneva, Switzerland, 2008.
9. *IEC 61400-21, Wind Turbine Generator Systems—Measurement and Assessment of Power Quality Characteristics of Grid Connected Wind Turbines*; IEC: Geneva, Switzerland, 2001.
10. Simonov, M.; Mussetta, M.; Grimaccia, F.; Leva, S.; Zich, R.E. Artificial Intelligence forecast of PV plant production for integration in smart energy systems. *Int. Rev. Electr. Eng.* **2012**, *7*, 3454–3460.
11. Mohan, N.; Undeland, T.M.; Robbins, W.P. *Power Electronics: Converters, Applications and Design*, 2nd ed.; Wiley & Sons: New York, NY, USA, 1995.
12. Klatt, M.; Dorado, A.; Meyer, J.; Schegner, P.; Backes, J.; Li, R. Power Quality Aspects of Rural Grids with High Penetration of Microgeneration, Mainly PV-Installations. In *Proceedings of the 21st International Conference on Electricity Distribution*, Frankfurt, Germany, 6–9 June 2011; pp. 1–4.
13. Tiam, T.Y.; Kirschen, D.S. Impact on the Power System of a Large Penetration of Photovoltaic Generation. In *Proceedings of the IEEE Power Engineering Society General Meeting*, Tampa, FL, USA, 24–28 June 2007; pp. 1–8.
14. Brenna, M.; Lazaroiu, G.C.; Superti-Furga, G.; Tironi, E. Bidirectional front-end converter for DG with disturbance insensitivity and islanding detection capability. *IEEE Trans. Power Del.* **2008**, *23*, 907–914.
15. *IEEE Standard 929-2000: IEEE Recommended Practice for Utility Interface of Photovoltaic (PV) Systems*; IEEE: Piscataway, NJ, USA, 2000.
16. Papaioannou, I.T.; Alexiadis, M.C.; Demoulias, C.S.; Labridis, D.P.; Dokopoulos, P.S. Modeling and field measurements of photovoltaic units connected to LV grid: Study of penetration scenarios. *IEEE Trans. Power Del.* **2011**, *26*, 979–987.
17. Chicco, G.; Schlabach, J.; Spertino, F. Characterisation and Assessment of the Harmonic Emission of Grid-Connected Photovoltaic Systems. In *Proceedings of the IEEE Power Tech Conference 2005*, Sankt Petersburg, Russia, 27–30 June 2005; pp. 1–7.